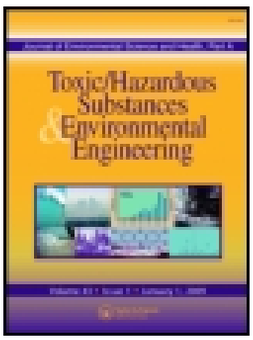

Taylor & Francis
Taylor & Francis Group

Journal of Environmental Science and Health, Part A
Toxic/Hazardous Substances and Environmental Engineering

ISSN: (Print) (Online) Journal homepage: https://www.tandfonline.com/loi/lesa20

Hepatic proteomic assessment of oral ingestion of titanium dioxide nano fiber (TDNF) in Sprague Dawley rats

Worlanyo E. Gato, Ji Wu, Isaac Appiah, Olivia Smith & Haresh Rochani

To cite this article: Worlanyo E. Gato, Ji Wu, Isaac Appiah, Olivia Smith & Haresh Rochani (2023): Hepatic proteomic assessment of oral ingestion of titanium dioxide nano fiber (TDNF) in Sprague Dawley rats, Journal of Environmental Science and Health, Part A, DOI: 10.1080/10934529.2022.2159733

To link to this article: https://doi.org/10.1080/10934529.2022.2159733

JOURNAL OF ENVIRONMENTAL SCIENCE AND HEALTH, PART A
https://doi.org/10.1080/10934529.2022.2159733

Hepatic proteomic assessment of oral ingestion of titanium dioxide nano fiber (TDNF) in Sprague Dawley rats

Worlanyo E. Gato[a], Ji Wu[a], Isaac Appiah[a], Olivia Smith[b], and Haresh Rochani[c]

[a]Department of Chemistry & Biochemistry, Georgia Southern University, Statesboro, Georgia, USA; [b]Department of Chemistry, Otterbein University, Westerville, Ohio, USA; [c]Department of Environmental Health and Biostatistics, Jiann-Ping Hsu College of Public Health, Georgia Southern University, Statesboro, Georgia, USA

ABSTRACT

Titanium dioxide nanofibers (TDNF) have been widely employed in pigments, sunscreens, paints, ointments, toothpaste and photocatalytic splitting of water. However, their potential toxicity has not been thoroughly examined. The goal of the present study is to examine hepatic effects associated with the ingestion of TDNF. TDNF was fabricated via electrospinning method and characterized. Six to seven weeks old male Sprague Dawley rats ingested (oral gavage) a total of 0 ppm, 40, 60 ppm TDNF for two weeks. After sacrifice, the liver was assessed for cellular effects using proteomic approach. The fibers diameter ranged from $0.18 - 0.29\,\mu$m, forming clusters and majority of the fibers were in the rutile phase. Proteomics assessment revealed more that more than 400 hundred proteins in the liver may be affected. These proteins are involved in such processes as catalysis of fatty acids by CoA, homocysteine metabolism, beta oxidation and the condensation of carbamoyl phosphate in the urea cycle among others. Further analysis of the protein associations showed that 325 biological processes, 140 molecular functions and 70 cellular components appear to be affected from the ingestion of TNDF. Quantitative analysis of specific mRNA transcripts indicated CMBL, GSTM1 and SDS were differentially expressed.

ARTICLE HISTORY
Received 18 August 2022
Accepted 12 December 2022

KEYWORDS
Protetomics; 2-Aminoanthracene (2AA); Titanium dioxide nanofibers (TDNF); liver; gene expression

Introduction

Nanomaterials are a class of substances with at least one dimension measurement that falls in the range of 1-100 nm long. Their small size endows these materials with properties that vary from their bulk counterparts, such as large surface-to-volume ratios, high porosity, conductivity, and fine crystalline structure.[1] There are also quantum effects in play with nanomaterials' size, which affect their chemical reactivity and mechanical, optical, electric, and magnetic properties, making them useful in applications from drug delivery to electronics to cosmetics.[2,3] Specifically, titanium dioxide nanofibers (TDNF) have been widely employed in pigments, sunscreens, paints, capacitors, gas sensors, and the photocatalytic splitting of water because of their high refractive index, chemical inertia, and semiconductor ability, among others.[3] The synthesis of these nanomaterials is achieved via electrospinning, which controls the size and shape of the nanofibers and ensures a narrow size distribution of the nanofibers. This control allows for more accurate analysis on how the physical properties of these nanofibers affect the chemical properties, with different sizes possibly leading to different properties that can then be selected for or against in trials and production.[4–6]

Although TDNF has great applications in the physical and chemical sciences and engineering, there are concerns over their potential toxicity. For example, a recent study involving TDNF exposure in an *in vitro* system found a significant increase in cytotoxicity and oxidative stress that was caused by higher levels of exposure.[7] As a bulk compound, titanium dioxide (TD) has been used for decades as it is considered safe even for consumption due to its chemical inertia. These smaller particles are also then easier to shed into the environment from everyday wear and tear of the TD products, where they can be ingested by humans. Besides this easier route of exposure, the smaller scale of these compounds may also play a role in increasing their toxicity as their physical and chemical properties are affected by size. [8]

Studies such as Brand et al. [9] and Hong and Zhang[10] have found evidence of oxidative stress, inflammation, and even liver damage as a result of TD exposure in rodent models and humans.[9,10] Previous studies under Gato and Wu[11] revealed a pattern of liver toxicity when rats were exposed to TDNF by the presence of gene expression related to inflammation, apoptosis, oxidative stress, and different signaling pathways.[11,12] Further studies are vital for exploring the effects of TDNF when exposed to animal models through dermal contact, as TDNF is often used in sunscreen and consumers should be aware of any possible adverse health effects, even those as seemingly minor as inflammation. The goal of the present study was thus to investigate the hepatic effects of ingesting TiO_2 NF in male Sprague Dawley rats by

CONTACT Worlanyo E. Gato wgato@georgiasouthern.edu Department of Chemistry and Biochemistry, Georgia Southern University, Statesboro, GA 30458, USA

Supplemental data for this article can be accessed online at https://doi.org/10.1080/10934529.2022.2159733.

first characterizing the previously synthesized TDNF using SEM and PXRD analysis and proteomic analysis.

The field of proteomics deals with the large-scale study of proteins and their interactions. This field provides a means of addressing major challenges about the health of organisms. Proteomics technology is useful in identifying altered proteins in relation to biological processes and molecular pathways as result of exposure to various environmentally relevant materials including nanomaterials. These alterations have provided the reasonable basis to understand the underlying mechanisms that may cause the occurrence of toxicity, diseases and the discovery of new biomarkers[13–15] to improve disease diagnosis and management. It is a particularly important research tool because most diseases are manifested at the level of protein activity, which allows for the rapid identification and quantification of proteins. Over the last decade proteomics has found a lot of applications across various fields including toxicology, biology, food safety and medicine among others.[13,16–18]

Material and methods

Synthesis and characterization of TiO_2 nano fiber (TDNF)

The fabrication of titanium dioxide nanofibers (TiO_2 NF) began with mixing ~1 gram of polyvinylpyrrolidone (PVP) with 10 mL of ethanol. In a separate container ~3 grams of TiIP (titanium iso-propoxide) was mixed with 5 mL of ethanol and 3 mL of Acetic Acid. These solutions were vortexed separately for ~ 30 minutes to ensure thorough mixing. The solutions were then added together and vortexed again for another 5 minutes. This mixture was then sonicated for 20 minutes before electrospinning. Once the gelation of the intended nanofiber was completed, it was ready for electrospinning. The parameters of electrospinning were as follows: the distance from the end of the syringe to the grounding aluminum collector was 12-15 cm. The pumping rate of sol-gel solution was 5 mL/hr. The applied DC voltage was 25 kV. Once all the sol-gel solution had been electrospun, fabricated fibers were left overnight for complete gelation. These nanofibers were annealed at ~565 °C in air for roughly 12 hours.

The morphology and structure of the fibers were characterized using scanning electron microscopy (SEM). The SEM used for nanofiber imaging was the JEOL model JSM-6610LV, with a tungsten filament, up to 30 kV and ×300,000 magnification, set at high vacuum.

Finally, the powder x-ray diffraction (PXRD) was used to determine the crystalline structure of the nanofiber. The PXRD instrument used for compound analysis was the PANalytical Empyrean, at acceleration voltage of 45 kV and current of 40 mA, with an X-Celerator and Bragg-Benton container for the Cu metal tube. The $2\theta\Theta$ range for the instrument measurement was 10 to 90°, the step rate was 0.1°/s, and the wavelength of Kα was 1.541 Ð.

Animal study

Male Sprague Dawley rats were purchased from Taconic Bioscience Inc., Hudson NY. The animals were 6-7 weeks old at the time of treatment. Animals are randomly assigned into total ingestion concentration of 0 ppm (control - FC), 40 ppm (low concentration - FLC) and 60 ppm (medium concentration - FMC) for two weeks. There were four animals in each treatment group. The rats were euthanized, and blood was collected by cardiac puncture at the expiration of treatment period. Excised livers were immediately frozen in liquid nitrogen and stored in −80 °C until analysis.

The animals were housed at the Georgia Southern University Animal Facility (1176 A Biological Sciences Fieldhouse). This facility is accredited by the Association for Assessment and Accreditation of Laboratory Animal Care (AAALAC). Rats were treated according to the principles outlined in the ILAR's (Institute for Laboratory Animal Research) Guide for Care and Use of Laboratory Animals. IACUC (institutional animal care and use committee) protocols were reviewed and approved by the Institutional Animal Care and Use Committee (IACUC protocol# I15002). The protocol was careful to minimize the number of animals employed in the research as well as reducing animal discomfort as much as possible.

Total protein extraction and ID gel electrophoresis

Total protein was extracted from liver tissues using Qproteome Mammalian Protein Prep Kit (Qiagen, Valencia 2006). Approximately 40 mg of tissues were lysed in 1 mL mammalian cell lysis buffer including 10 µl protease inhibitor and 1 U benzonase nuclease. This was followed by tissues disruption for 30 s at medium speed in 15 mL propylene centrifuge tube. Samples were then transferred into 2 mL precooled microcentrifuge tubes and centrifuged at 7800 rpm for 10 minutes. The supernatant was filtered through Whatman 0.2 µm PVDF Filter Media and concentrated via 3 K Amicon centrifugal filter device for 20 minutes. Samples were then aliquoted and stored at −20 °C.

Protein samples were diluted with Laemmli sample buffer in a ratio of 1:1. The Laemmli buffer was prepared by adding 25 µlL β-mercaptoethanol to 475 µlL Laemmli sample buffer. The protein-Laemmli mixture was vortexed briefly and heated for 5 minutes at 95 °C. Fifteen microliters of the mixture along with a molecular weight marker were loaded onto a mini-protean TGX precast gel. The gel was run at constant 200 V and 50 mA using 1X Tris/glycine/SDS gel running buffer for 35 minutes. Gel was then pulled off the cassette and rinsed three times for 5 minutes each with distilled water. The gel was stained with 50 mL of Bio-Safe Coomassie G-250 stain for 1 hour with gentle shaking before being de-stained with a mixture of acetic acid and methanol overnight. The gels were washed again with high purity MilliQ for 30 minutes and imaged. The bands of each column of the gel were cut out of the gel and suspended in distilled water.

Proteomic analysis

The gel bands were excised from the 1 D gel groups and shipped to the Proteomic and Mass Spectrometry Core Facility, University of Georgia, Athens GA for analysis. Then, gel bands were processed for in-gel trypsin digestion and

peptide extraction using the following protocol: destaining, reduction and alkylation, in-gel digestion and extraction. The supernatant was analyzed directly without further processing.

With respect to the mass spectrometry analysis, tryptic peptides from in-gel digestion were analyzed by Proxeon nanoLC HPLC system is coupled to a Thermo-Fisher LTQ Orbitrap Elite. Peptide fragments were loaded directly to the analytical column that is self-packed with C18, similar to Jupiter Proteo resin (Phenomenex). The preferred method was to measure both MS and MS/MS in the orbitrap at 120,000 and at 3,000, respectively. LC/MS runs were searched against Rat of SwissProt database using Proteome Discoverer with Mascot (Matrix Sciences) to identify unique peptide signatures.

Bulk protein data analysis

Bulk protein data were combined to find the same accessions in the treatment groups. Then, the same accessions in treatments groups were analyzed. Data were analyzed using SAS 9.3 statistical software package for Windows (SAS Institute Inc., Cary, NC, USA). Descriptive analysis was applied to variable 'score' by treatment group. The dependent variables were also compared descriptively across groups to illustrate temporal trends. The treatment effect is analyzed using general linear model. The treatment effect is statistically significant ($p < 0.05$). And the scores for each accession is different ($p < 0.05$).

Analysis of protein associations via DAVID

DAVID (database for annotation, visualization and integrated discovery) was employed to analyze protein relationships within the samples. The Gene Ontology (GO) comparison tool provides the opportunity to show the relationship between and the association of peptides with respect to each other in functional and biochemical pathways.[19] This tool organizes transcripts into hierarchical categories via biological process, molecular function, and cellular components. Proteins accession numbers from were imported into DAVID bioinformatics tool for analysis.

Gene expression

To further examine the effects of oral ingestion of TDNF, six genes noted to play vital roles were selected to be analyzed extensively through the process of quantitative real-time polymerase chain reaction (qRT-PCR). These six genes include: CPS1, EPHX1, GSTM1, CMBL, CCT4, and SDS (Table 1). Total RNA was extracted from liver tissues using the Qiagen's RNeasy Plus Universal Mini kit and protocol. Total RNA samples were reverse transcribed and combined with appropriate primer sets followed by quantitative PCR measurements using BioRad's CFX instrument. Relative gene expression of these samples between the control, and treated rats were analyzed.

Results

Characterization of TDNF

Shown in Figure 1A is the image of SEM micrograph, revealing that nanofibers have diameters in the range of 0.18 μm to 0.29 μm. The image also shows clusters of fibers overlaying one another. PXRD was used to determine the crystal structure of the fibers. TDNF crystal structure is shown in Figure 1B. The image indicates that TDNF material to be in the rutile phase of titanium dioxide, with some traces of anatase.[20]

Bulk protein analysis and associations via DAVID

To examine the effects of oral ingestion of TDNF on the liver of rats, mass spectrometry was then employed to identify specific protein signatures that might be essential in understanding the toxicity of TDNF. There were more than 400 unique protein signatures identified with varied abundance (supplemental material). Though further analysis

Table 1. A select proteins were selected for further analysis via quantitative PCR. Forward and reverse primers of these transcripts are shown in this table.

Gene	Brief Description	Primer Sequence
CPS1	provides instructions for making the enzyme carbamoyl phosphate synthetase I. This enzyme participates in the urea cycle, a series of reactions that occurs in liver cells.	Forward CTGAGGGATGCTGATCCTATTC Reverse GGATTCTGTCCTTCCTGAGATG
EPHX1	a critical biotransformation enzyme that converts epoxides from the degradation of aromatic compounds to trans-dihydrodiols which can be conjugated and excreted from the body.	Forward GTACCCTCACTTCAAGACCAAG Reverse CCCACGTTCCATGTAGGAATAG
GSTM1	encodes a cytoplasmic glutathione S-transferase that belongs to the mu class. Th mu class of enzymes functions in the detoxification of electrophilic compounds, including carcinogens	Forward TTGAGAAGCAGAAGCCAGAG Reverse AGAGAACCACAGTGCAGAAG
CMBL	a cysteine hydrolase of the dienelactone hydrolase family that is highly expressed in liver cytosol	Forward TTGTGCATCGGAAGAGAGAAG Reverse GAATCTAGCTGGTCCCTGAATG
CCT4	assists the folding of newly translated polypeptide substrates through multiple rounds of ATP-driven release and rebinding of partially folded intermediate forms.	Forward GATCCGCTTCAGCAACATTTC Reverse CACCAGCTCACAGTCATCTATC
SDS	encodes one of three enzymes that are involved in metabolizing serine and glycine.	Forward CAGCAATTGGGAGACTGAGA Reverse GGTGCTTGGCACAACAATAG

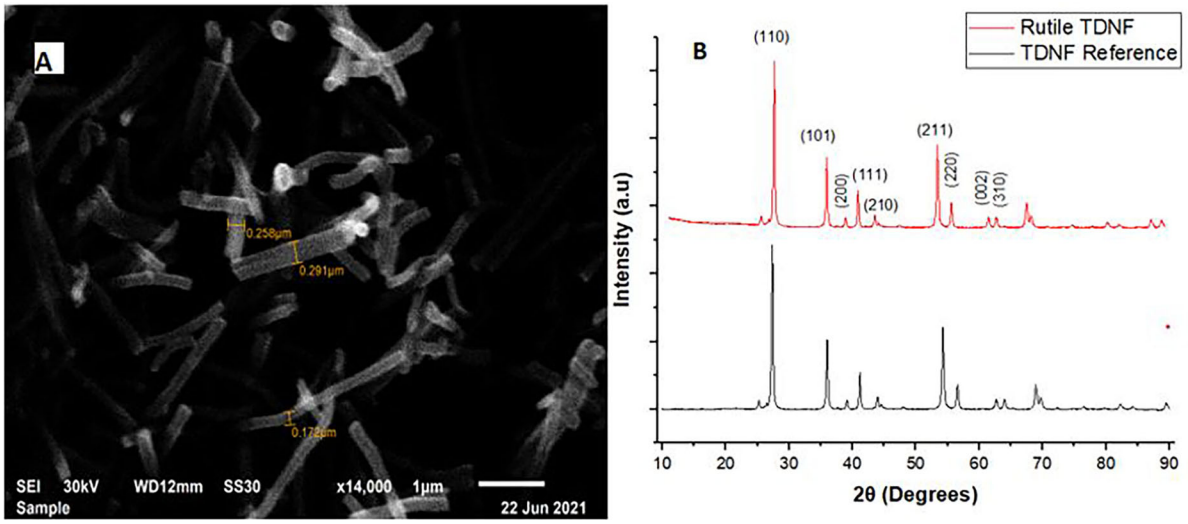

Figure 1. The structure and morphology of TDNF material was examined using A: SEM (show nanofiber diameters ranging from 0.18 to 0.29 μm) and B: PXRD (profile matches for the synthesized material to be in the rutile phase of titanium dioxide, with some traces of anatase).

showed possible significant changes, it was difficult to relate those changes to specific biological processes and mechanisms (Table 2).

Results from DAVID analysis categorized the observed effects into biological process, cellular components and molecular function. Biological process was the most affected followed by molecular function and then cellular component (Figure 2). Some of the biological processes include; oxidation reduction (103 proteins), response to extracellular stimulus (25 proteins), response to drugs (32 proteins) and carboxylic acid catabolic process (37 proteins) among others. In the case of cellular components, categories include mitochondrion (143 proteins), cytosol (114 proteins), membrane-enclosed lumen (89 proteins) and organelle envelope (68 proteins) among others. Finally, the molecular functions had among its categories, cofactor binding (68 proteins), nucleotide binding (93 proteins), lipid binding (28 proteins) and antioxidant activity (11 proteins) (Table 3). Further, DAVID showed some pathways that were affected MF). Some of the pathways affected include fatty acid metabolism, PPAR signaling pathways, glycolysis/gluconeogenesis, glutathione metabolism and ribosome (Table 4).

Table 2. A segment of the protein analysis table showing accession number, estimates of random effects and significant estimated values. More than 400 proteins were identified.

Solution for Random Effects

Effect	Accession	Estimate	Std Err, Pred	DF	t Value	Pr > |t|
Accession	A7VJC2	−0.3952	0.2110	862	−1.87	0.0615
Accession	B0BNE5	0.6024	0.1392	862	4.33	<.0001
Accession	B0BNN3	−0.9768	0.2739	862	−3.57	0.0004
Accession	B3DMA2	−1.9577	0.4258	862	−4.60	<.0001
Accession	D3ZAF6	−1.9577	0.4258	862	−4.60	<.0001
Accession	O09171	2.3571	0.08348	862	28.24	<.0001
Accession	O35077	1.5602	0.1007	862	15.49	<.0001
Accession	O35244	0.7029	0.1340	862	5.25	<.0001
Accession	O35763	−2.3850	0.5121	862	−4.66	<.0001
Accession	O35952	−2.1513	0.4634	862	−4.64	<.0001
Accession	O70199	−0.3952	0.2110	862	−1.87	0.0615
Accession	O70351	0.7690	0.1307	862	5.88	<.0001
Accession	O70490	−2.3850	0.5121	862	−4.66	<.0001
Accession	O88618	0.5717	0.1409	862	4.06	<.0001
Accession	O88767	0.5239	0.1435	862	3.65	0.0003
Accession	O88989	0.7165	0.1333	862	5.37	<.0001
Accession	P00173	0.9120	0.1241	862	7.35	<.0001
Accession	P00176	−1.3082	0.3182	862	−4.11	<.0001
Accession	P00388	−0.6200	0.2332	862	−2.66	0.0080
Accession	P00406	−0.05500	0.1820	862	−0.30	0.7626
Accession	P00481	1.8772	0.09261	862	20.27	<.0001
Accession	P00502	1.6808	0.09742	862	17.25	<.0001

Gene expression

The gene expression of a select mRNA transcripts show the over-expression of SDS, GSTM1, and CMBL. On the contrary, CCT4, CPS1 and EPHX1expression were not significantly altered (Figure 3).

Discussion

Titanium dioxide nanomaterials have a wide variety of applications spanning electronic and cosmetic fields.[3,21] As a result, studying the toxicity of TiO_2 nanofiber is essential to fully understanding adverse health implications from exposure to these materials. The analysis of protein associations will be useful to note pathways and particular proteins that will be most affected by the ingestion of TiO_2 nanofiber.

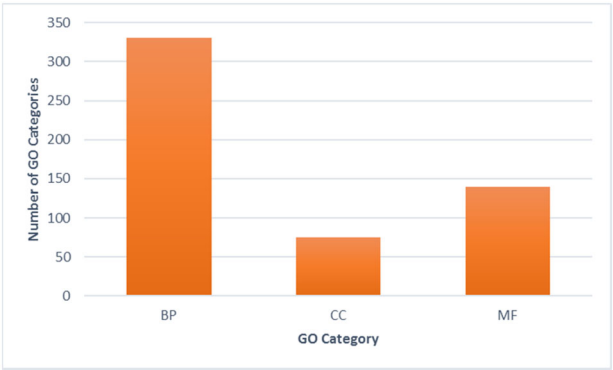

Figure 2. Distribution of protein categories by gene ontology (GO). This is subdivided into 3 categories: Biological Processes (BP), Cellular Component (CC), and Molecular Function (MF).

Table 3. Functional annotation of protein list showing gene ontology (GO) categories of biological process (BP), cellular component (CC) and molecular function (MF). GO categories significantly ($p < 0.01$) observed to be affected by TDNF ingestion.

Category	Term	Count	p-value
BP	oxidation reduction	103	2.30E-55
	organic acid catabolic process	37	2.10E-32
	carboxylic acid catabolic process	37	2.10E-32
	fatty acid beta-oxidation	14	3.30E-14
	lipid oxidation	16	4.90E-14
	cellular amino acid derivative metabolic process	24	8.00E-11
	response to inorganic substance	30	9.10E-11
	lipid modification	16	1.10E-10
	response to drug	32	5.70E-10
	oxidoreduction coenzyme metabolic process	14	5.70E-10
	monosaccharide biosynthetic process	12	8.30E-10
	cellular respiration	15	8.30E-10
	acetyl-CoA catabolic process	9	7.30E-08
	translation	33	9.60E-08
	response to metal ion	20	2.00E-07
	oxidative phosphorylation	13	2.80E-07
	gluconeogenesis	8	1.40E-06
	response to extracellular stimulus	25	1.40E-06
	response to nutrient levels	24	1.50E-06
	glycolysis	10	2.10E-06
CC	mitochondrion	143	1.20E-50
	cytosol	114	7.40E-34
	organelle inner membrane	56	2.30E-28
	mitochondrial lumen	44	9.20E-28
	mitochondrial matrix	44	9.20E-28
	microsome	49	7.70E-25
	vesicular fraction	49	3.00E-24
	organelle envelope	68	5.30E-24
	microbody	27	3.20E-19
	peroxisome	27	3.20E-19
	cell fraction	81	7.80E-18
	endoplasmic reticulum	66	1.20E-14
	cytosolic ribosome	18	4.90E-14
	soluble fraction	37	6.70E-13
	pigment granule	19	2.90E-12
	melanosome	19	2.90E-12
	ribosomal subunit	20	3.00E-12
	membrane-enclosed lumen	81	2.10E-11
	mitochondrial proton-transporting ATP synthase complex	9	5.50E-08
	ribosome	31	6.30E-08
	microbody part	11	2.50E-07
	peroxisomal part	11	2.50E-07
	proton-transporting ATP synthase complex	9	5.80E-07
	endoplasmic reticulum part	25	1.10E-06
	ribonucleoprotein complex	35	9.10E-06
	outer membrane	13	4.70E-05
	extrinsic to membrane	23	1.50E-04
	nucleoid	7	1.80E-04
	mitochondrial proton-transporting ATP synthase complex, coupling factor F(o)	5	6.30E-04
	large ribosomal subunit	7	6.30E-04
	mitochondrial outer membrane	10	8.20E-04
MF	cofactor binding	68	4.70E-42
	coenzyme binding	51	2.80E-31
	electron carrier activity	37	6.30E-18
	iron ion binding	39	1.20E-15
	FAD binding	20	7.60E-14
	heme binding	22	8.70E-10
	glutathione transferase activity	11	9.30E-10
	tetrapyrrole binding	22	1.80E-09
	hydro-lyase activity	12	4.30E-09
	transferase activity, transferring alkyl or aryl (other than methyl) groups	13	8.90E-09
	vitamin B6 binding	13	4.40E-08
	pyridoxal phosphate binding	13	4.40E-08
	nucleotide binding	93	1.30E-07
	antioxidant activity	11	2.20E-07
	structural constituent of ribosome	27	2.80E-07
	NADP or NADPH binding	10	3.50E-07
	identical protein binding	40	4.60E-07
	oxidoreductase activity, acting on the CH-NH group of donors	8	1.50E-06
	acyl-CoA dehydrogenase activity	7	1.90E-06
	lipid binding	28	3.90E-06
	amino acid binding	12	7.00E-06
	steroid binding	10	1.90E-05

(*continued*)

Table 3. Continued.

Category	Term	Count	p-value
	intramolecular oxidoreductase activity, interconverting keto- and enol-groups	5	2.00E-05
	peroxiredoxin activity	5	2.00E-05
	protein homodimerization activity	24	3.10E-05
	transaminase activity	7	3.10E-05
	monocarboxylic acid binding	10	4.60E-05
	peroxidase activity	7	1.00E-04
	purine nucleotide binding	71	1.40E-04
	oxygen binding	7	1.60E-04
	adenyl nucleotide binding	61	1.70E-04
	glutathione binding	5	1.70E-04
	hydrogen ion transporting ATP synthase activity, rotational mechanism	5	1.70E-04
	structural molecule activity	33	1.80E-04
	nucleoside binding	62	1.90E-04
	drug binding	10	2.60E-04
	purine nucleoside binding	61	2.60E-04
	fatty acid binding	8	2.70E-04
	glucuronosyltransferase activity	5	3.50E-04
	monovalent inorganic cation transmembrane transporter activity	11	3.80E-04
	nucleobase binding	4	4.10E-04
	protein disulfide isomerase activity	4	4.10E-04
	intramolecular oxidoreductase activity, transposing S-S bonds	4	4.10E-04
	ADP binding	6	4.60E-04
	steroid dehydrogenase activity, acting on the CH-OH group of donors, NAD or NADP as acceptor	6	4.60E-04
	proton-transporting ATPase activity, rotational mechanism	5	4.80E-04
	C-acyltransferase activity	5	4.80E-04
	iron-sulfur cluster binding	8	6.50E-04
	oxidoreductase activity, acting on the aldehyde or oxo group of donors, NAD or NADP as acceptor	8	8.10E-04

Table 4. Significant ($p < 0.05$) pathways found through DAVID analysis to be important in understanding the hepatic toxicity from the ingestion of TDNF. Proteins involved in each pathway ranges from 6 to 34 in number.

Pathway Accession	Number of Proteins	p-value
Drug metabolism	34	2.20E-26
Metabolism of xenobiotics by cytochrome P450	27	3.50E-20
Fatty acid metabolism	22	4.10E-18
Ribosome	28	4.20E-17
Valine, leucine and isoleucine degradation	21	8.40E-16
Arginine and proline metabolism	19	4.10E-12
Tryptophan metabolism	17	1.30E-11
Butanoate metabolism	15	3.20E-11
Ascorbate and aldarate metabolism	11	3.80E-10
beta-Alanine metabolism	12	5.00E-10
Propanoate metabolism	13	7.20E-09
Glutathione metabolism	15	1.90E-08
Citrate cycle (TCA cycle)	12	2.80E-08
Pyruvate metabolism	13	6.30E-08
Limonene and pinene degradation	8	9.10E-08
Retinol metabolism	15	1.90E-07
Glycolysis / Gluconeogenesis	17	6.20E-07
Lysine degradation	12	1.10E-06
PPAR signaling pathway	15	2.10E-06
Phenylalanine metabolism	8	2.60E-06
Glyoxylate and dicarboxylate metabolism	7	5.40E-06
Glycine, serine and threonine metabolism	10	6.80E-06
Tyrosine metabolism	10	1.20E-05
Drug metabolism	11	1.70E-05
Alanine, aspartate and glutamate metabolism	9	3.50E-05
Histidine metabolism	8	5.80E-05
Steroid hormone biosynthesis	10	8.90E-05
Cysteine and methionine metabolism	9	1.10E-04
Primary bile acid biosynthesis	6	3.50E-04
Nitrogen metabolism	7	3.90E-04
Parkinson's disease	17	5.20E-04

The size distribution of the fibers is critical to the chemical and physical properties of the nanofibers and thus, the toxicity likely to be experienced from exposure. Examination of the fibers via SEM after electrospinning showed the diameters to range from 0.18 to 0.29 μm. Fibers were also formed clusters. Further structural analysis showed that the fibers were in the rutile phase. The chromatogram indicated 20 matches in the peak list for rutile position and peak height out of 21 total peaks for the sample titanium dioxide. When compared and matched with the anatase phase, there were only a handful of matching peaks at small, uneven heights corresponding to the anatase. Analysis using the PXRD instrument software revealed peak matching percentages, with TDNF coming in at a 95% match for rutile TD, indicating high purity of the sample. The matching positions are at positions 27, 36, 39, 41, 44, 63, 64, 68, and 69. The peak heights vary in terms of how well they match between the sample and the literature data for some of the peaks but are within one order of magnitude.[20]

To explore the effects of TDNF ingestion in Sprague Dawley rats, a proteomics approach was used. Proteomics is a useful tool to evaluating the complete structure and function of proteins in an organism.[22] More than 400 hundred proteins were identified to be involved in TDNF effects in the liver. Some of these include Acyl-coenzyme A synthetase ACSM2, mitochondrial (Accession#: O70490), Betaine–homocysteine S-methyltransferase 1 (Accession#: O09171), Acyl-CoA dehydrogenase family member 11 (Accession#: B3DMA2) and Ornithine transcarbamylase, mitochondrial precursor (Accession#: P00481) among many more. These proteins are involved in such processes as catalysis of fatty acids by CoA, homocysteine metabolism, beta oxidation and the condensation of carbamoyl phosphate in the urea cycle.[23–25]

Though, identification of individual proteins provides some insight into TDNF ingestion, grouping the proteins into aggregates and functional biological processes and functions will provide much clearer insight. Using DAVID bioinformatics tool,[19] individual proteins were grouped into associations referred to as gene ontology (GO) categories including functional biological process (BP), cellular components (CC) and molecular function (MF). GO categories

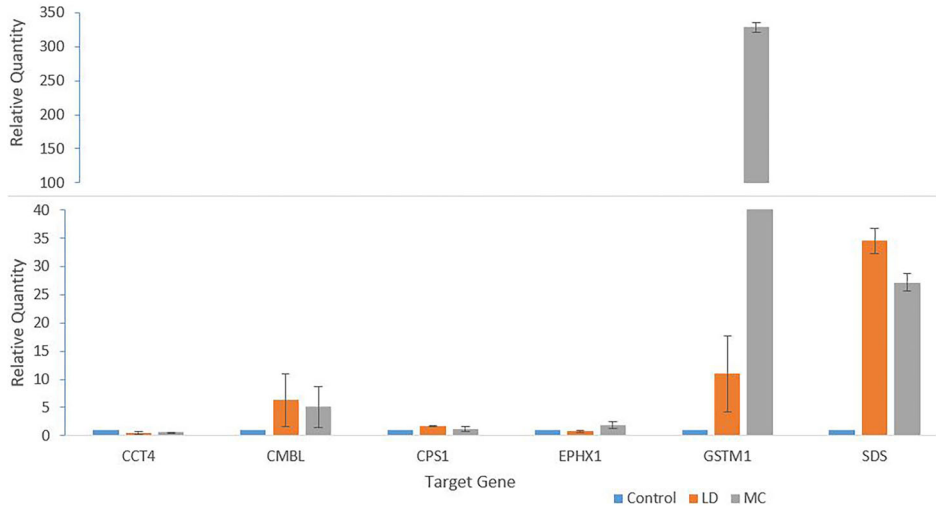

Figure 3. The gene expression of a select proteins chosen from the bulk protein data. mRNA levels in control, low dose (40 ppm) and medium dose (60 ppm) titanium dioxide nanofiber (TDNF) treatment groups were quantified.

included 325 biological processes, 140 molecular functions and 70 cellular components. The BP category showed oxidation reduction as the most represented. This was followed up by organic and carboxylic acid catabolism, response to drug, translation and response to extracellular stimulus. These processes are essential for the metabolic health of the cell. In the case of the molecular function categories, cofactor & coenzyme, lipid, nucleotide binding seemed to show the most appearance. Cellular components including the mitochondrion, cytosol, organelle envelope and membrane-enclosed lumen among others were highly represented in the gene ontology category. It appears that TDNF ingestion affects the metabolic acidity in the liver of Sprague Dawley rats. To further understand these protein associations via DAVID, pathway analysis was also performed. More than 30 pathways were affected by TDNF ingestion. Some of these were; drug metabolism, PPAR signaling pathway, and metabolism of xenobiotics by cytochrome p450. These pathways similar to the gene ontology categories, seem to play essential roles in metabolism within the liver. For instance the peroxisome proliferator-activated receptors (PPARs) are considered as nuclear receptor proteins that modulate transcription through the regulation of gene expression. [26]

A few of these proteins were examined via quantitative polymerase chain reaction. The genes quantified included CPS1 (essential for carbamoyl phosphate synthesis [27]); EPHX1 (converts epoxides to be excreted from the body [28]); GSTM1 (protein that detoxifies electrophilic compounds [29]); CMBL (key enzyme necessary for the biodegradation of xenobiotics [30]; CCT4 (chaperonin essential for cell cycle protein degradation [31]) and SDS (encodes for enzymes that metabolizing serine and glycine [32]). It appears CCT4, CPS1 and EPHX1 were not differentially expressed. In comparison to controls, CMBL, GSTM1 and SDS were differentially expressed. Though gene expression cannot be directly correlated with protein activity, however the differential expression of these genes in treated groups may indicate TDNF effects as it relates to the metabolism of xenobiotics and amino acids.

Conclusion

This paper investigated the hepatic proteomic effects of oral ingestion of titanium dioxide nanofibers. Titanium dioxide nanofibers have been used a variety of applications. Understanding the toxicological implications of these materials is critical for avoiding adverse health effects associated with their use. Analysis of the structure of the materials show that the diameter ranged from $0.18 - 0.29\,\mu$m, forming clusters and majority of the fibers were in the rutile phase. To understand toxicity effects, nanofibers were ingested by Sprague Dawley rats. Proteomics assessment revealed more that more than 400 hundred proteins in the liver that may be affected. These proteins are involved in such processes as catalysis of fatty acids by CoA, homocysteine metabolism, beta oxidation and the condensation of carbamoyl phosphate in the urea cycle among others. Further analysis of the protein associations by DAVID bioinformatics tool showed that gene ontology (GO) categories including functional biological process (BP), cellular components (CC) and molecular function (MF). GO categories included 325 biological processes, 140 molecular functions and 70 cellular components appear to be affected from the ingestion of TNDF. Quantitative analysis of specific mRNA transcripts indicated CMBL, GSTM1 and SDS were differentially expressed. In conclusion, it appears that the ingestion of TDNF produced mild toxicological effects in the liver of Sprague Dawley rats.

Acknowledgements

The authors acknowledge the assistance of Mr. Christopher Mays and Ms. Kayla Anderson for taking care of the rats. We are also thankful to Mr. Craig Banks, the animal facility manager for his assistance with the animal study. The Research Project was partially or fully sponsored by Georgia Southern University Office of Research and Economic Development.

Disclosure statement

No potential conflict of interest was reported by the authors.

Data availability statement (DAS)

Raw data were generated at University of Georgia Mass Spectrometry Facility. Derived data supporting the findings of this study are available from the corresponding author [WEG] on request.

Funding

The author(s) reported there is no funding associated with the work featured in this article.

References

[1] Khan, I.; Saeed, K.; Khan, I. Nanoparticles: Properties, Applications and Toxicities. *Arab. J. Chem.* **2019**, *12*, 908–931. DOI: 10.1016/j.arabjc.2017.05.011.

[2] Testino, A.; Bellobono, I. R.; Buscaglia, V.; Canevali, C.; D'Arienzo, M.; Polizzi, S.; Scotti, R.; Morazzoni, F. Optimizing the Photocatalytic Properties of Hydrothermal TiO2 by the Control of Phase Composition and Particle Morphology. A Systematic Approach. *J. Am. Chem. Soc.* **2007**, *129*, 3564–3575. DOI: 10.1021/ja067050+.

[3] Stephen, L. Titanium dioxide versatile solid crystalline: An overview. In *Assorted Dimensional Reconfigurable Materials*, Rajendra Dongre, Dilip Peshwe, Eds. IntechOpen, **2020**. DOI: 10.5772/intechopen.92056.

[4] McCann, J. T.; Li, D.; Xia, Y. Electrospinning of Nanofibers with Core-Sheath, Hollow, or Porous Structures. *J. Mater. Chem.* **2005**, *15*, 735–738. DOI: 10.1039/b415094e.

[5] Kanani, A. G.; Bahrami, S. H. Review on Electrospun Nanofibers Scaffold and Biomedical Applications. *Trends Biomater. Artif. Organs* **2010**, *24*, 93–115.

[6] Zumeta, I.; Díaz, D.; Santiago, P. Synthesis of TiO2 Nanoparticles with Narrow Size Distribution and Their Evaluation in the Photocatalytic Oxidative Degradation of Bis (4-Nitrophenyl) Phosphate. *J. Phys. Chem. C* **2010**, *114*, 11381–11389. DOI: 10.1021/jp1021399.

[7] Ramkumar, K. M.; Manjula, C.; GnanaKumar, G.; Kanjwal, M. A.; Sekar, T. V.; Paulmurugan, R.; Rajaguru, P. Oxidative Stress-Mediated Cytotoxicity and Apoptosis Induction by TiO2 Nanofibers in HeLa Cells. *Eur. J. Pharm. Biopharm.* **2012**, *81*, 324–333. DOI: 10.1016/j.ejpb.2012.02.013.

[8] Skocaj, M.; Filipic, M.; Petkovic, J.; Novak, S. Titanium Dioxide in Our Everyday Life; is It Safe? *Radiol. Oncol.* **2011**, *45*, 227–247. DOI: 10.2478/v10019-011-0037-0.

[9] Brand, W.; Peters, R. J.; Braakhuis, H. M.; Maślankiewicz, L.; Oomen, A. G. Possible Effects of Titanium Dioxide Particles on Human Liver, Intestinal Tissue, Spleen and Kidney after Oral Exposure. *Nanotoxicology* **2020**, *14*, 985–1007. DOI: 10.1080/17435390.2020.1778809.

[10] Hong, J.; Zhang, Y.-Q. Murine Liver Damage Caused by Exposure to Nano-Titanium Dioxide. *Nanotech* **2016**, *27*, 112001. DOI: 10.1088/0957-4484/27/11/112001.

[11] Gato, W. E.; Hunter, D. A.; Byrd, I. C.; Mays, C. A.; Yau, W.; Wu, J. Assessment of the Short-Term Toxicity of TiO2 Nanofiber in Sprague Dawley Rats. *Environ. Toxicol.* **2017**, *32*, 1775–1783. DOI: 10.1002/tox.22400.

[12] Bartel, L. K.; Hunter, D. A.; Anderson, K. B.; Yau, W.; Wu, J.; Gato, W. E. Short-Term Evaluation of Hepatic Toxicity of Titanium Dioxide Nanofiber (TDNF). *Drug Chem. Toxicol.* **2019**, *42*, 35–42.

[13] Campos, A.; Tedesco, S.; Vasconcelos, V.; Cristobal, S. Proteomic Research in Bivalves: Towards the Identification of Molecular Markers of Aquatic Pollution. *J. Proteomics* **2012**, *75*, 4346–4359. DOI: 10.1016/j.jprot.2012.04.027.

[14] Chan, P. P.; Wasinger, V. C.; Leong, R. W. Current Application of Proteomics in Biomarker Discovery for Inflammatory Bowel Disease. *World J. Gastrointest. Pathophysiol.* **2016**, *7*, 27–37. DOI: 10.4291/wjgp.v7.i1.27.

[15] Causey, D. R.; Pohl, M. A.; Stead, D. A.; Martin, S. A.; Secombes, C. J.; Macqueen, D. J. High-Throughput Proteomic Profiling of the Fish Liver following Bacterial Infection. *BMC Genom.* **2018**, *19*, 1–17.

[16] Rodrigues, P. M.; Schrama, D.; Campos, A.; Osório, H.; Freitas, M. Applications of Proteomics in Aquaculture. In *Agricultural Proteomics* Volume 1; Springer: Cham Switzerland, **2016**; pp 175–209.

[17] De Felice, B.; Parolini, M. Can Proteomics Be Considered as a Valuable Tool to Assess the Toxicity of Nanoparticles in Marine Bivalves? *JMSE* **2020**, *8*, 1033. DOI: 10.3390/jmse8121033.

[18] Lam, L.; Lind, J.; Semsarian, C. Application of Proteomics in Cardiovascular Medicine. *Int. J. Cardiol.* **2006**, *108*, 12–19. DOI: 10.1016/j.ijcard.2006.01.002.

[19] Huang, D. W.; Sherman, B. T.; Tan, Q.; Kir, J.; Liu, D.; Bryant, D.; Guo, Y.; Stephens, R.; Baseler, M. W.; Lane, H. C.; Lempicki, R. A. DAVID Bioinformatics Resources: expanded Annotation Database and Novel Algorithms to Better Extract Biology from Large Gene Lists. *Nucleic Acids Res.* **2007**, *35*, W169–W175.

[20] Thamaphat, K.; Limsuwan, P.; Ngotawornchai, B. J. A.; Resources, N. Phase Characterization of TiO2 Powder by XRD and TEM. *Agric Nat, Resour* **2008**, *42*, 357–361.

[21] Mu, L.; Sprando, R. L. J. P. r Application of Nanotechnology in Cosmetics. *Pharm Res* **2010**, *27*, 1746–1749. DOI: 10.1007/s11095-010-0139-1.

[22] Al-Amrani, S.; Al-Jabri, Z.; Al-Zaabi, A.; Alshekaili, J.; Al-Khabori, M. Proteomics: Concepts and Applications in Human Medicine. *WJBC* **2021**, *12*, 57–69. DOI: 10.4331/wjbc.v12.i5.57.

[23] Gerhard, D. S.; Wagner, L.; Feingold, E. A.; Shenmen, C. M.; Grouse, L. H.; Schuler, G.; Klein, S. L.; Old, S.; Rasooly, R.; Good, P. The Status, Quality, and Expansion of the NIH Full-Length cDNA Project: The Mammalian Gene Collection (MGC). *Genome Res* **2004**, *14*, 2121–2127.

[24] Kikuchi, M.; Hatano, N.; Yokota, S.; Shimozawa, N.; Imanaka, T.; Taniguchi, H. Proteomic Analysis of Rat Liver Peroxisome: presence of Peroxisome-Specific Isozyme of Lon Protease. *J. Biol. Chem.* **2004**, *279*, 421–428. DOI: 10.1074/jbc.M305623200.

[25] McDowall, S.; Heeswijck, R. v.; Hoogenraad, N. Site-Directed Mutagenesis of Arg60 and Cys271 in Ornithine Transcarbamylase from Rat Liver. *Protein Eng. Des. Sel.* **1990**, *4*, 73–77. DOI: 10.1093/protein/4.1.73.

[26] Ahmadian, M.; Suh, J. M.; Hah, N.; Liddle, C.; Atkins, A. R.; Downes, M.; Evans, R. M. PPARγ Signaling and Metabolism: The Good, the Bad and the Future. *Nat. Med.* **2013**, *19*, 557–566. DOI: 10.1038/nm.3159.

[27] Choi, Y.; Oh, A.; Lee, Y.; Kim, G.-H.; Choi, J.-H.; Yoo, H.-W.; Lee, B. H. Unfavorable Clinical Outcomes in Patients with Carbamoyl Phosphate Synthetase 1 Deficiency. *Clin. Chim. Acta* **2022**, *526*, 55–61. DOI: 10.1016/j.cca.2021.11.029.

[28] Gautheron, J.; Morisseau, C.; Chung, W. K.; Zammouri, J.; Auclair, M.; Baujat, G.; Capel, E.; Moulin, C.; Wang, Y.; Yang, J.; et al. EPHX1 Mutations Cause a Lipoatrophic Diabetes Syndrome Due to Impaired Epoxide Hydrolysis and Increased Cellular Senescence. *Elife* **2021**, *10*, e68445. DOI: 10.7554/eLife.68445.

[29] Wang, S.; Fan, Z. The Role of GSTM1 Gene Polymorphism in Pathophysiology, Evaluation, and Management of Constipation of Anorectal Outlet Obstruction. *Cell Mol. Biol (Noisy-le-Grand)* **2021**, *67*, 163–167.

[30] Ishizuka, T.; Fujimori, I.; Kato, M.; Noji-Sakikawa, C.; Saito, M.; Yoshigae, Y.; Kubota, K.; Kurihara, A.; Izumi, T.; Ikeda, T.; Okazaki, O. Human Carboxymethylenebutenolidase as a Bioactivating Hydrolase of Olmesartan Medoxomil in Liver and Intestine. *J. Biol. Chem.* **2010**, *285*, 11892–11902. DOI: 10.1074/jbc.M109.072629.

[31] Li, F.; Liu, C.-S.; Wu, P.; Ling, A.-S.; Pan, Q.; Li, X.-N. CCT4 Suppression Inhibits Tumor Growth in Hepatocellular Carcinoma by Interacting with Cdc20. *Chin. Med. J. (Engl)* **2021**, *134*, 2721–2729.

[32] Sun, L.; Li, X.; Dong, Y.; Yang, M.; Liu, Y.; Han, X.; Zhang, X.; Pang, H.; Rao, Z. Crystallization and Preliminary Crystallographic Analysis of Human Serine Dehydratase. *Acta Crystallogr. D Biol. Crystallogr.* **2003**, *59*, 2297–2299.